

THE NUMERICAL METHODS FOR SOLVING OF THE ONE-DIMENSIONAL ANOMALOUS REACTION-DIFFUSION EQUATION¹

MAREK BŁASIK

*Silesian University of Technology, Department of Mathematics Applications and Methods for Artificial Intelligence, Poland
e-mail: marek.blasik@polsl.pl*

This paper presents numerical methods for solving the one-dimensional fractional reaction-diffusion equation with the fractional Caputo derivative. The proposed methods are based on transformation of the fractional differential equation to an equivalent form of an integro-differential equation. The paper proposes an improvement of the existing implicit method, and a new explicit method. Stability and convergence tests of the methods were also conducted.

Keywords: fractional derivatives and integrals, integro-differential equations, numerical methods, anomalous diffusion

1. Introduction

Anomalous diffusion refers to a type of random motion or transport process that deviates from classical, normal, or Brownian diffusion behavior. In classical diffusion, particles move randomly and independently, following a Gaussian distribution. Anomalous diffusion is characterized by a non-Gaussian distribution (Metzler and Klafter, 2000, 2004;), and may involve mechanisms such as hindered motion or trapping.

The importance of anomalous diffusion in research lies in its prevalence in various natural and artificial systems as well as its implications for understanding complex physical (Solomon *et al.*, 1993; Weeks *et al.*, 1996; Kosztolowicz *et al.*, 2005a, 2005b) and environmental (Humphries *et al.*, 2010) processes.

The anomalous reaction-diffusion equation is a mathematical model that describes spatiotemporal evolution of a quantity such as concentration in a system where both diffusion and reaction processes are affected by anomalous behavior. This equation is commonly used to study how concentrations of substances change over time and space due to both diffusion and chemical reactions (Owolabi *et al.*, 2020; Haq *et al.*, 2021).

A number of numerical methods have been proposed to solve the anomalous reaction-diffusion equation, recent results devoted to this problem are contained in the papers (Coronel-Escamilla *et al.*, 2018; Liu *et al.*, 2015; Pradip and Prasad Goura, 2023; Saad and Gomez-Aguilar, 2018; Sandip and Srinivasan, 2023; Saxena *et al.*, 2015).

The article presents novel numerical techniques designed to solve the one-dimensional fractional reaction-diffusion equation with the fractional Caputo derivative. In particular, the paper introduces improvements to the existing implicit method and introduces an entirely new explicit method. Comprehensive tests to evaluate the stability (the algorithm presented in the paper is a novel approach) and convergence of these new methods are also presented.

¹Paper presented during PCM-CMM 2023, Gliwice, Poland

2. Preliminaries

This Section includes definitions of the left-sided Riemann-Liouville integral and the left-sided Caputo derivative. Both definitions, along with the composition rule of the aforementioned operators, are taken from the monograph (Kilbas *et al.*, 2006) and written in the context of subdiffusion, i.e., for $\alpha \in (0, 1]$.

Definition 1. *The left-sided Riemann-Liouville integral of order α , denoted as I_{0+}^α , is given by the following formula for $\operatorname{Re}(\alpha) \in (0, 1]$*

$$I_{0+}^\alpha f(t) := \frac{1}{\Gamma(\alpha)} \int_0^t \frac{f(\tau) d\tau}{(t-\tau)^{1-\alpha}} \quad (2.1)$$

where Γ is the Euler gamma function.

Definition 2. *Let $\operatorname{Re}(\alpha) \in (0, 1]$. The left-sided Caputo derivative of order α is given by the formula*

$${}^C D_{0+}^\alpha f(t) := \begin{cases} \frac{1}{\Gamma(1-\alpha)} \int_0^t \frac{f'(\tau)}{(t-\tau)^\alpha} d\tau & \text{for } 0 < \alpha < 1 \\ \frac{df(t)}{dt} & \text{for } \alpha = 1 \end{cases} \quad (2.2)$$

Property 1. *Let function $f \in C^1(0, T)$. Then, the composition rule for the left-sided Riemann-Liouville integral and the left-sided Caputo derivative is given as follows*

$$I_{0+}^\alpha {}^C D_{0+}^\alpha f(t) = f(t) - f(0) \quad (2.3)$$

The definition of the Mittag-Leffler function that is used in the remainder of this article is taken from the monograph (Podlubny, 1999).

Definition 3. *Let $\gamma > 0$. The one-parameter Mittag-Leffler function is given as the following series*

$$E_\gamma(z) = \sum_{k=0}^{\infty} \frac{z^k}{\Gamma(\gamma k + 1)} \quad (2.4)$$

Definition 4. *Let $\Pi = \{(x, t) : x \in [0, L]; t \in [0, T]\}$ be a continuous region of solutions for the partial differential equation. Then the set $\bar{\Pi} = \{(x_i, t_j) \in \Pi : x_i = i\Delta x, i \in \{0, 1, \dots, m\}, \Delta x = L/m; t_j = j\Delta t, j \in \{0, 1, \dots, n\}; \Delta t = T/n\}$ we call the rectangular regular mesh described by the set of nodes.*

3. Mathematical formulation and numerical solution of the problem

Consider the one-dimensional anomalous reaction-diffusion equation

$${}^C D_{0+,t}^\alpha U(x, t) = D_\alpha \frac{\partial^2 U(x, t)}{\partial x^2} + Q_\alpha(x, t, U) \quad 0 \leq x \leq L \quad 0 \leq t \leq T \quad (3.1)$$

supplemented with the boundary conditions

$$U(0, t) = f(t) \quad U(L, t) = g(t) \quad 0 \leq t \leq T \quad (3.2)$$

and the initial condition

$$U(x, 0) = h(x) \quad 0 \leq x \leq L \quad (3.3)$$

3.1. Explicit numerical scheme

The implicit numerical method (Błasiak, 2021) has some limitations, namely, it cannot solve an equation in which the source term is of the form $Q_\alpha(x, t, U)$. Therefore, in this Subsection, an explicit method is proposed that will work when the source term depends on the function U . A key role in the proposed approach is played by Property 1, which makes it possible to transform Eq. (3.1) into an equivalent integro-differential equation

$$U(x, t) = U(x, 0) + \frac{D_\alpha}{\Gamma(\alpha)} \int_0^t \frac{1}{(t - \tau)^{1-\alpha}} \frac{\partial^2 U(x, \tau)}{\partial x^2} d\tau + \frac{1}{\Gamma(\alpha)} \int_0^t \frac{Q_\alpha(x, \tau, U)}{(t - \tau)^{1-\alpha}} d\tau \quad (3.4)$$

Further considerations will be carried out by taking into account the grid of nodes specified in Definition 4. For every node in the grid, we ascertain discrete representation of the integral kernel in the integrals mentioned in Eq. (3.4) on the right-hand side. To achieve this, we estimate the solution U by employing a constant function between two successive nodes in relation to the variable t (Diethelm, 2010) as follows $\bar{U}(x, t) = U(x, t_j)$ for $t_j \leq t \leq t_{j+1}$, $j = 0, \dots, n - 1$. Hence, we have

$$\frac{D_\alpha}{\Gamma(\alpha)} \int_0^{t_k} \frac{1}{(t_k - \tau)^{1-\alpha}} \frac{\partial^2 U(x, \tau)}{\partial x^2} d\tau \approx \frac{D_\alpha}{\Gamma(\alpha)} \int_0^{t_k} \frac{1}{(t_k - \tau)^{1-\alpha}} \frac{\partial^2 \bar{U}(x, \tau)}{\partial x^2} d\tau \quad (3.5)$$

From the additivity of the integral with respect to the integration interval and the approximation of the second order derivative of the function U with respect to the spatial variable by the differential quotient, we obtain

$$\begin{aligned} \frac{D_\alpha}{\Gamma(\alpha)} \int_0^{t_k} \frac{1}{(t_k - \tau)^{1-\alpha}} \frac{\partial^2 \bar{U}(x, \tau)}{\partial x^2} d\tau &= \frac{D_\alpha}{\Gamma(\alpha)} \sum_{j=0}^{k-1} \int_{t_j}^{t_{j+1}} \frac{1}{(t_k - \tau)^{1-\alpha}} \frac{\partial^2 U(x, t_j)}{\partial x^2} d\tau \\ &= \frac{D_\alpha}{\Gamma(\alpha)} \sum_{j=0}^{k-1} \frac{(t_k - t_j)^\alpha - (t_k - t_{j+1})^\alpha}{\alpha} \frac{\partial^2 U(x, t_j)}{\partial x^2} \\ &= \frac{D_\alpha \Delta t^\alpha}{\Gamma(\alpha + 1)} \sum_{j=0}^{k-1} [(k - j)^\alpha - (k - j - 1)^\alpha] \frac{\partial^2 U(x, t_j)}{\partial x^2} \\ &= \frac{D_\alpha \Delta t^\alpha}{\Gamma(\alpha + 1)} \sum_{j=0}^{k-1} [(k - j)^\alpha - (k - j - 1)^\alpha] \frac{U_{i-1,j} - 2U_{i,j} + U_{i+1,j}}{(\Delta x)^2} \\ &= D_\alpha \sum_{j=0}^{k-1} \frac{r_{j,k}}{\Delta x^2} (U_{i-1,j} - 2U_{i,j} + U_{i+1,j}) \end{aligned}$$

where the discrete form of the kernel of the left-sided Riemann-Liouville integral is given by the formula

$$r_{j,k} = \frac{\Delta t^\alpha}{\Gamma(\alpha + 1)} [(k - j)^\alpha - (k - j - 1)^\alpha] \quad (3.6)$$

Repeating the same discretization for the second integral on the right-hand side of equation (3.4), we get

$$\frac{1}{\Gamma(\alpha)} \int_0^t \frac{Q_\alpha(x, \tau, U)}{(t - \tau)^{1-\alpha}} d\tau \approx \frac{1}{\Gamma(\alpha)} \int_0^t \frac{\bar{Q}_\alpha(x, \tau, U)}{(t - \tau)^{1-\alpha}} d\tau \quad (3.7)$$

and sequentially

$$\begin{aligned}
\frac{1}{\Gamma(\alpha)} \int_0^t \frac{\bar{Q}_\alpha(x, \tau, U)}{(t-\tau)^{1-\alpha}} d\tau &= \frac{1}{\Gamma(\alpha)} \sum_{j=0}^{k-1} \int_{t_j}^{t_{j+1}} \frac{1}{(t_k-\tau)^{1-\alpha}} Q_\alpha(x, t_j, U) d\tau \\
&= \frac{1}{\Gamma(\alpha)} \sum_{j=0}^{k-1} \int_{t_j}^{t_{j+1}} \frac{(t_k-t_j)^\alpha - (t_k-t_{j+1})^\alpha}{\alpha} Q_\alpha(x, t_j, U) d\tau \\
&= \frac{\Delta t^\alpha}{\Gamma(\alpha+1)} \sum_{j=0}^{k-1} [(k-j)^\alpha - (k-j-1)^\alpha] Q_\alpha(x_i, t_j, U_{i,j}) = \sum_{j=0}^{k-1} r_{j,k} Q_\alpha(x, t_j, U)
\end{aligned} \tag{3.8}$$

Finally, we get an explicit numerical scheme

$$U_{i,k} = U_{i,0} + D_\alpha \sum_{j=0}^{k-1} \frac{r_{j,k}}{\Delta x^2} (U_{i-1,j} - 2U_{i,j} + U_{i+1,j}) + \sum_{j=0}^{k-1} r_{j,k} Q_{\alpha i,j} \tag{3.9}$$

3.2. Implicit numerical scheme

The numerical method proposed in this Subsection is a modification of the method presented in the paper (Błasiak, 2021). The main change consists in a different way of discretizing the source term of the equation. The expression $\sum_{j=0}^k w_{j,k} Q_{\alpha i,j}$ has been replaced by $\sum_{j=0}^{k-1} r_{j,k} Q_{\alpha i,j}$, look at the last component of equation (3.10). We can write the improved implicit numerical scheme in the form

$$\begin{aligned}
& - \frac{D_\alpha w_{k,k}}{(\Delta x)^2} U_{i-1,k} + \left(1 + \frac{2D_\alpha w_{k,k}}{(\Delta x)^2}\right) U_{i,k} - \frac{D_\alpha w_{k,k}}{(\Delta x)^2} U_{i+1,k} \\
& = U_{i,0} + \sum_{j=0}^{k-1} \frac{D_\alpha w_{j,k}}{(\Delta x)^2} (U_{i-1,j} - 2U_{i,j} + U_{i+1,j}) + \sum_{j=0}^{k-1} r_{j,k} Q_{\alpha i,j}
\end{aligned} \tag{3.10}$$

where

$$w_{j,k} := \frac{(\Delta t)^\alpha}{\Gamma(2+\alpha)} \begin{cases} (\alpha+1-k)k^\alpha + (k-1)^{\alpha+1} & j=0 \\ (k-j+1)^{\alpha+1} - 2(k-j)^{\alpha+1} + (k-j-1)^{\alpha+1} & 0 < j < k \\ 1 & j=k \end{cases} \tag{3.11}$$

Note that now we do not need to know the value of the source term at the k -th time layer. So the scheme can be written as a system of $n-1$ algebraic equations in the matrix form

$$\mathbf{A} \mathbf{U}_k = \mathbf{B} \tag{3.12}$$

where matrices **A** and **B** are defined as

$$\mathbf{A} = \begin{bmatrix} 1+2a & -a & 0 & 0 & \cdots & 0 & 0 & 0 \\ -a & 1+2a & -a & 0 & \cdots & 0 & 0 & 0 \\ 0 & -a & 1+2a & -a & \cdots & 0 & 0 & 0 \\ \vdots & \vdots & \vdots & \vdots & \ddots & \vdots & \vdots & \vdots \\ 0 & 0 & 0 & -a & 1+2a & -a & 0 & 0 \\ \vdots & \vdots & \vdots & \vdots & \ddots & \vdots & \vdots & \vdots \\ 0 & 0 & 0 & 0 & \cdots & -a & 1+2a & -a \\ 0 & 0 & 0 & 0 & \cdots & 0 & -a & 1+2a \end{bmatrix}$$

$$\mathbf{B} = \begin{bmatrix} b_1 + aU_{0,k} \\ b_2 \\ b_3 \\ \vdots \\ b_i \\ \vdots \\ b_{m-2} \\ b_{m-1} + aU_{m,k} \end{bmatrix}$$

The elements of matrices **A** and **B** are defined by the formulas

$$a := \frac{D_\alpha w_{k,k}}{(\Delta x)^2}$$

$$b_i := U_{i,0} + \sum_{j=0}^{k-1} \frac{D_\alpha w_{j,k}}{\Delta x^2} (U_{i-1,j} - 2U_{i,j} + U_{i+1,j}) + \sum_{j=0}^{k-1} r_{j,k} Q_{\alpha i,j}$$

4. Numerical examples

This Section presents numerical results which are compared with a closed exact solution. In the calculations, the following form of the analytical solution was adopted

$$U(x, t) = \frac{1}{2} \sin(x) E_\alpha(t^\alpha) \tag{4.1}$$

From the fact of invariance of the Mittag-Leffler function with respect to the left-sided Caputo derivative, the form of the source term is derived. Thus, we define the initial boundary value problem as

$${}^C D_{0+,t}^\alpha U(x, t) = \frac{\partial^2 U(x, t)}{\partial x^2} + 2U(x, t) \quad 0 \leq x \leq \frac{\pi}{2} \quad t \geq 0 \tag{4.2}$$

supplemented with the boundary conditions

$$U(0, t) = 0 \quad U\left(\frac{\pi}{2}, t\right) = \frac{1}{2} E_\alpha t^\alpha \quad t \geq 0 \tag{4.3}$$

and the initial condition

$$U(x, 0) = \frac{1}{2} \sin x \quad 0 \leq x \leq \frac{\pi}{2} \tag{4.4}$$

where the generalized diffusion coefficient D_α is equal to one. In the calculations, the following mesh parameters were assumed: $T = 0.1$, $L = \pi/2$, $m, n \in \{25, 50, 100, 200\}$, and the order of the left-sided Caputo derivative $\alpha \in \{0.25, 0.5, 0.75, 1\}$.

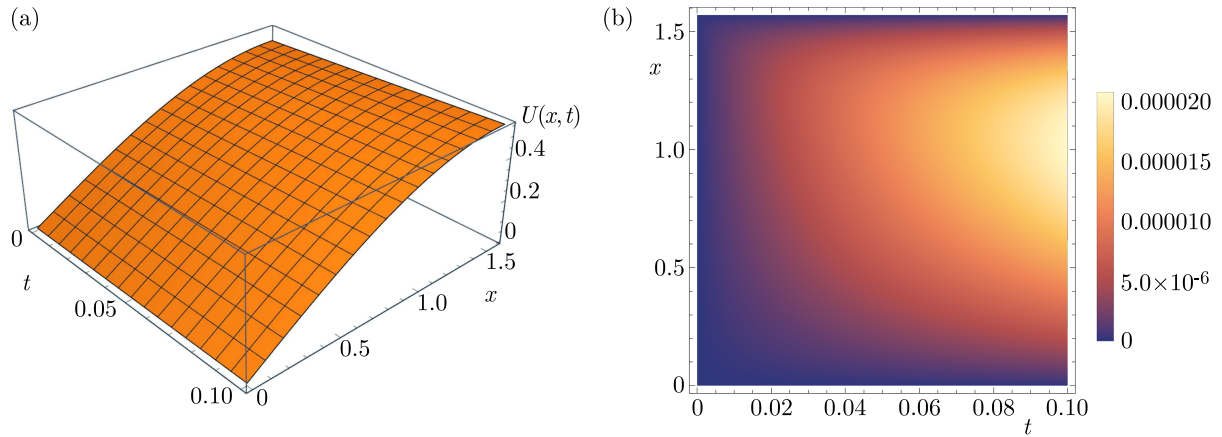


Fig. 1. The numerical solution of the initial-boundary value problem for $\alpha = 1$ (a). The absolute error generated by the numerical method for $\alpha = 1$ (b)

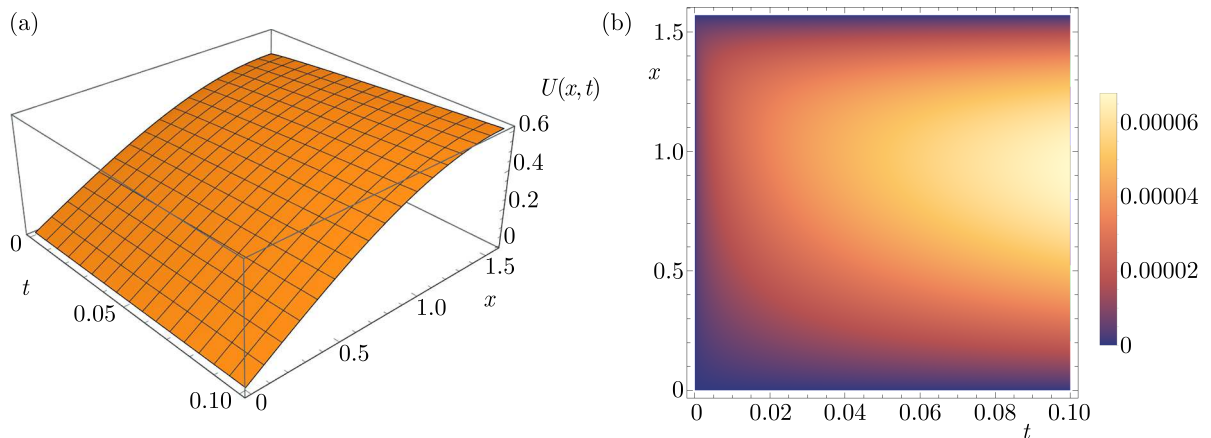


Fig. 2. The numerical solution of the initial-boundary value problem for $\alpha = 75$ (a). The absolute error generated by the numerical method for $\alpha = 75$ (b)

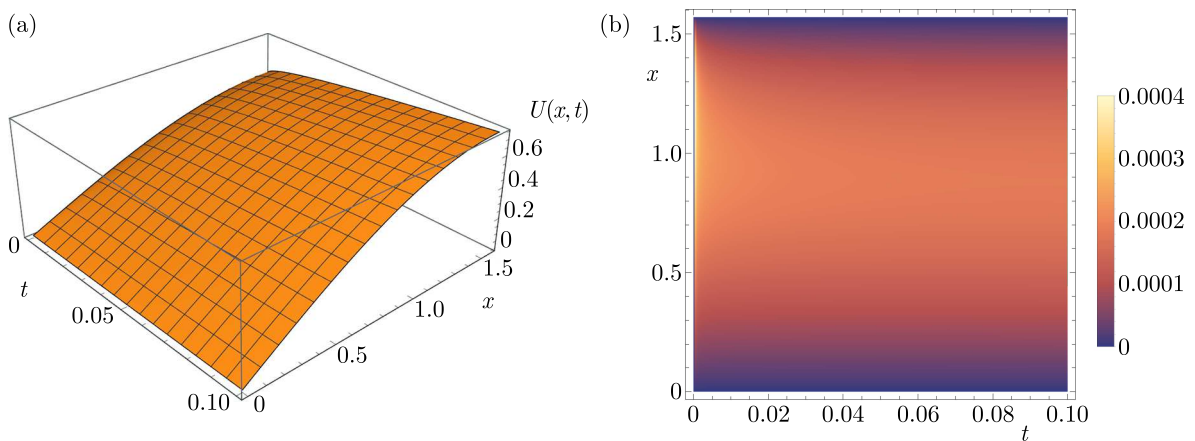


Fig. 3. The numerical solution of the initial-boundary value problem for $\alpha = 0.5$ (a). The absolute error generated by the numerical method for $\alpha = 0.5$ (b)

Figures 1-4, part (a), show the numerical solutions of Eq. (4.2)-(4.4) obtained by the implicit method for four different values of the order of the left-sided Caputo derivative. Part (b) presents the absolute error generated by the proposed method resulting from validation of the numerical scheme with exact solution Eq. (4.1). For large values of the order of the left-sided Caputo

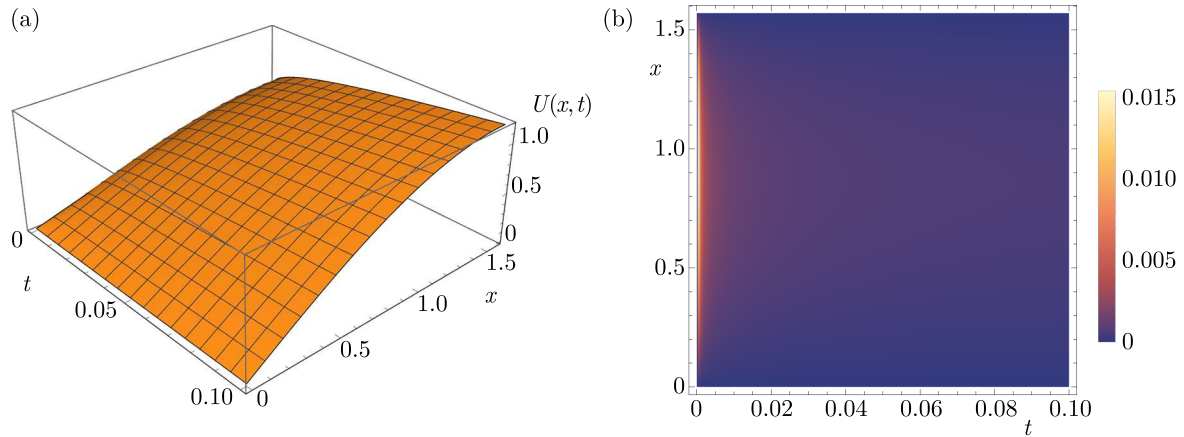


Fig. 4. The numerical solution of the initial-boundary value problem for $\alpha = 0.25$ (a). The absolute error generated by the numerical method for $\alpha = 0.25$ (b)

derivative: $\alpha = 1$ and $\alpha = 0.75$, we observe its smallest value near the boundary conditions, for $x = 0$ and $x = \pi/2$. We also notice that the error accumulates and reaches the maximum value for $t = 0.1$. In the case of $\alpha = 0.5$ and $\alpha = 0.25$, the numerical scheme generates the largest errors for small values of the variable t .

Tables 1-4 present the average absolute errors generated by the implicit numerical scheme for sixteen grid variants and four values of the order of the left-sided Caputo derivative. The results clearly show that the order of the derivative has a significant effect on the accuracy of the numerical method, and the average absolute error is negatively correlated with it.

Table 1. The average absolute error generated by the numerical method for $\alpha = 1$

$n \backslash m$	25	50	100	200
25	$4.801 \cdot 10^{-5}$	$5.237 \cdot 10^{-5}$	$5.376 \cdot 10^{-5}$	$5.424 \cdot 10^{-5}$
50	$2.191 \cdot 10^{-5}$	$2.57 \cdot 10^{-5}$	$2.681 \cdot 10^{-5}$	$2.715 \cdot 10^{-5}$
100	$8.81 \cdot 10^{-6}$	$1.232 \cdot 10^{-5}$	$1.328 \cdot 10^{-5}$	$1.356 \cdot 10^{-5}$
200	$2.247 \cdot 10^{-6}$	$5.609 \cdot 10^{-6}$	$6.505 \cdot 10^{-6}$	$6.749 \cdot 10^{-6}$

Table 2. The average absolute error generated by the numerical method for $\alpha = 0.75$

$n \backslash m$	25	50	100	200
25	$2.298 \cdot 10^{-4}$	$2.415 \cdot 10^{-4}$	$2.457 \cdot 10^{-4}$	$2.474 \cdot 10^{-4}$
50	$1.099 \cdot 10^{-4}$	$1.191 \cdot 10^{-4}$	$1.221 \cdot 10^{-4}$	$1.231 \cdot 10^{-4}$
100	$5.02 \cdot 10^{-5}$	$5.815 \cdot 10^{-5}$	$6.049 \cdot 10^{-5}$	$6.124 \cdot 10^{-5}$
200	$2.049 \cdot 10^{-5}$	$2.782 \cdot 10^{-5}$	$2.985 \cdot 10^{-5}$	$3.044 \cdot 10^{-5}$

Table 3. The average absolute error generated by the numerical method for $\alpha = 0.5$

$n \backslash m$	25	50	100	200
25	$9.967 \cdot 10^{-4}$	$1.031 \cdot 10^{-3}$	$1.045 \cdot 10^{-3}$	$1.051 \cdot 10^{-3}$
50	$4.809 \cdot 10^{-4}$	$5.047 \cdot 10^{-4}$	$5.134 \cdot 10^{-4}$	$5.169 \cdot 10^{-4}$
100	$2.271 \cdot 10^{-4}$	$2.458 \cdot 10^{-4}$	$2.518 \cdot 10^{-4}$	$2.54 \cdot 10^{-4}$
200	$1.027 \cdot 10^{-4}$	$1.188 \cdot 10^{-4}$	$1.235 \cdot 10^{-4}$	$1.25 \cdot 10^{-4}$

Table 4. The average absolute error generated by the numerical method for $\alpha = 0.25$

$n \backslash m$	25	50	100	200
25	$4.952 \cdot 10^{-3}$	$5.084 \cdot 10^{-3}$	$5.144 \cdot 10^{-3}$	$5.171 \cdot 10^{-3}$
50	$2.401 \cdot 10^{-3}$	$2.482 \cdot 10^{-3}$	$2.515 \cdot 10^{-3}$	$2.529 \cdot 10^{-3}$
100	$1.147 \cdot 10^{-3}$	$1.201 \cdot 10^{-3}$	$1.222 \cdot 10^{-3}$	$1.23 \cdot 10^{-3}$
200	$5.359 \cdot 10^{-4}$	$5.784 \cdot 10^{-4}$	$5.922 \cdot 10^{-4}$	$5.972 \cdot 10^{-4}$

4.1. Convergence analysis

The convergence order is a measure of how quickly the grid method approaches the solution to the problem as the number of mesh nodes increases. The experimental convergence order is determined empirically by analyzing the rate at which the error decreases with each increase in the number of nodes. To determine the experimental order of convergence of the implicit numerical method, we use the formula (Gu *et al.*, 2021)

$$\text{EOC} = \log_2 \left(\frac{\frac{1}{(m+1)(n+1)} \sum_{j=0}^n \sum_{i=0}^m |U(x_i, t_j) - U_{i,j}^{m,n}|}{\frac{1}{(2m+1)(2n+1)} \sum_{j=0}^{2n} \sum_{i=0}^{2m} |U(x_i, t_j) - U_{i,j}^{2m,2n}|} \right) = \log_2 \left(\frac{\Delta U^{m,n}}{\Delta U^{2m,2n}} \right) \quad (4.5)$$

where $U(x_i, t_j)$ is the exact solution determined at node $(i\Delta x, j\Delta t)$, while $U_{i,j}^{m,n}$ represents the approximate solution calculated by the numerical method.

The data collected in Tables 5 and 6 clearly show that the experimental order of convergence tends to one very quickly, as m and n increases.

Table 5. Convergence order of the implicit numerical scheme for $\alpha \in \{1, 0.75\}$

n	m	$\alpha = 1$		$\alpha = 0.75$	
		$\Delta U^{m,n}$	EOC	$\Delta U^{m,n}$	EOC
25	25	$4.801 \cdot 10^{-5}$	–	$2.298 \cdot 10^{-4}$	–
50	50	$2.57 \cdot 10^{-5}$	0.902	$1.191 \cdot 10^{-4}$	0.948
100	100	$1.328 \cdot 10^{-5}$	0.953	$6.049 \cdot 10^{-5}$	0.977
200	200	$6.749 \cdot 10^{-6}$	0.977	$3.044 \cdot 10^{-5}$	0.991

Table 6. Convergence order of the implicit numerical scheme for $\alpha \in \{0.5, 0.25\}$

n	m	$\alpha = 1$		$\alpha = 0.75$	
		$\Delta U^{m,n}$	EOC	$\Delta U^{m,n}$	EOC
25	25	$9.967 \cdot 10^{-4}$	–	$4.952 \cdot 10^{-3}$	–
50	50	$5.047 \cdot 10^{-4}$	0.982	$2.482 \cdot 10^{-3}$	0.997
100	100	$2.518 \cdot 10^{-4}$	1.003	$1.222 \cdot 10^{-3}$	1.022
200	200	$1.25 \cdot 10^{-4}$	1.01	$5.972 \cdot 10^{-4}$	1.033

4.2. Stability analysis

During numerical tests, the explicit scheme defined by equation (3.9) showed features of conditional stability. For a certain ratio of the time and spatial step, it generated convergent solutions. After increasing the time step at a fixed spatial step, its divergence was observed. To determine the stability condition, an algorithm was proposed, which is described in this Section.

The stability condition of the numerical scheme is formulated for solution (4.1), which is monotonic in the region in which we solve the differential equation. Thus, considering any three

consecutive nodes with respect to the time or space variable, the value of the solution at the center node should not exceed the values obtained at neighboring nodes – this condition is written in the ninth line of the pseudocode. The algorithm can be described in several points:

- 1) we initiate the algorithm by specifying values: $\alpha = 1$, $t_{end} = 0.001$, $x_{start} = 0$, $x_{end} = \pi/2$, $m = 10$, $n = 10$,
- 2) we generate the solution by the explicit scheme and check the stability condition,
- 3) through the parameter $\lambda_t^2 = 0.90$, we modify the time step to obtain an unstable solution,
- 4) through the parameter $\lambda_t^1 = 0.99$, we slowly reduce the time step until the stability condition is fulfilled,
- 5) we write the spatial step and the largest possible time step that guarantee stability to the *result* list,
- 6) we reduce the spatial step with the parameter $\lambda_x = 0.93$ so that $x_{end} > x_{end}^*$, where $x_{end}^* = \pi/4$, and repeat steps 2-5.

The above-mentioned steps of the algorithm resulted in a set of points, which are presented in Fig. 5a. Then the approximation of points with the function $p_1 \Delta x^{p_2}$ was carried out. It should be noted that the fit of the function to the sets of points is almost perfect – the coefficient of determination after rounding to the fourth decimal place gives a value of one.

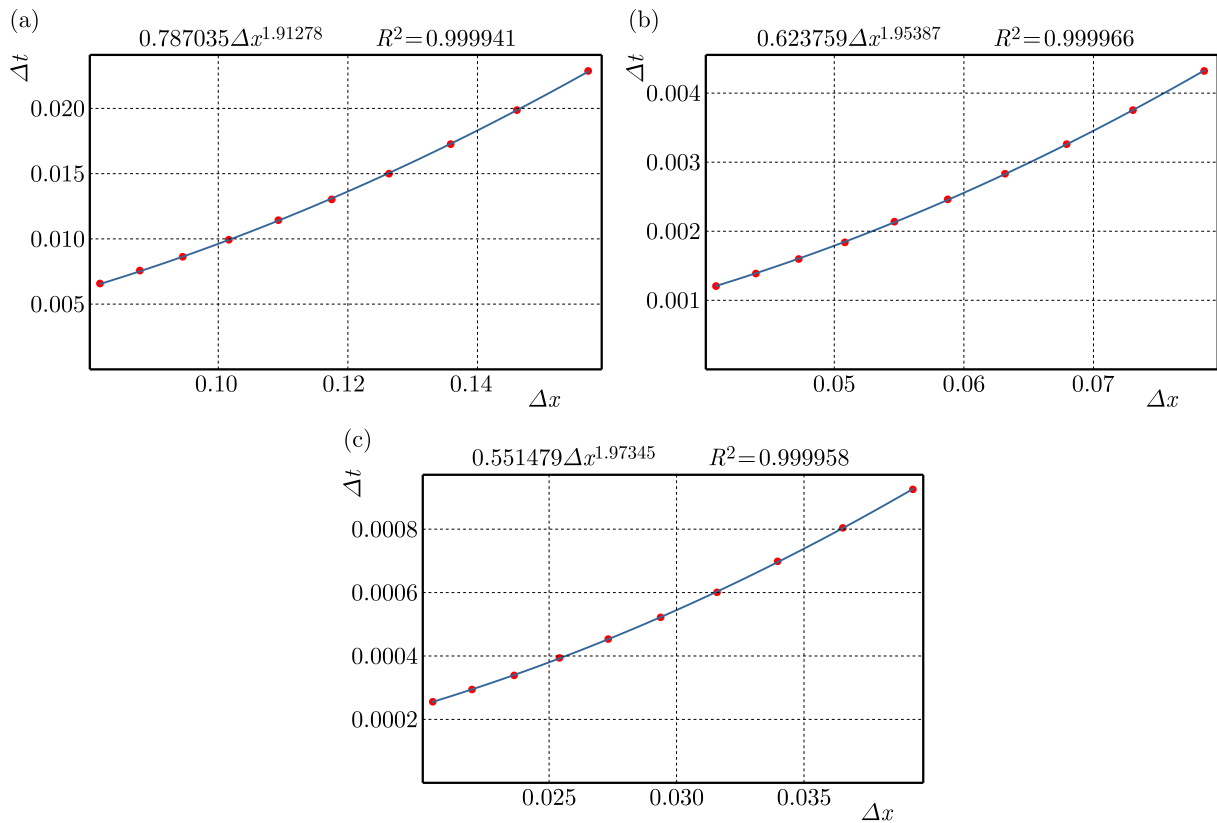


Fig. 5. Relationship between Δx and Δt for $\alpha = 1$ and (a) $m, n = 10$, (b) $m, n = 20$, (c) $m, n = 40$.

The obtained results are presented in Fig. 5 and Table 7. Analysis of the results leads to the following observations. For $\alpha = 1$ and increasing grid parameters m and n , $p_1 \rightarrow 0.5$ and $p_2 \rightarrow 2$, which is in accordance with the stability criterion for the explicit method for the classical diffusion equation where the relationship $\Delta t \leq 0.5 \Delta x^2$ occurs. Analysis of the results in the other cases of Table 7 leads to a more general condition in the form of $\Delta t \leq \delta_\alpha \Delta x^{2/\alpha}$.

Algorithm 1: Algorithm to test stability

Input : Initial values of: $\alpha, t_{end}, x_{start}, x_{end}, x_{end}^*, \lambda_x, \lambda_t^2, \lambda_t^1, m, n$
Output: List of points: *result*

```

1 while  $x_{end} > x_{end}^*$  do
2    $sta \leftarrow 0$ ;
3    $counter \leftarrow 1$ ;
4   while  $sta \neq 1$  do
5     Implicit_scheme( $\alpha, t_{end}, x_{start}, x_{end}, m, n$ );
6      $stop \leftarrow 0$ ;
7     for  $j \leftarrow 1$  to  $n - 1$  do
8       for  $i \leftarrow 1$  to  $m - 1$  do
9         if  $\left( \left| \frac{U_{i-1,j} + U_{i+1,j}}{2} - U_{i,j} \right| < \frac{1}{2} |U_{i+1,j} - U_{i-1,j}| \right)$  and
           $\left( \left| \frac{U_{i,j-1} + U_{i,j+1}}{2} - U_{i,j} \right| < \frac{1}{2} |U_{i,j+1} - U_{i,j-1}| \right)$  then
10          |  $sta \leftarrow 1$ ;
11          | end
12          | else
13          |    $sta \leftarrow 0$ ;
14          |    $stop \leftarrow 1$ ;
15          |   Break;
16          | end
17        end
18      end
19      if  $stop == 1$  then
20        | Break;
21      end
22    end
23    if  $sta == 1$  and  $counter == 1$  then
24      |  $t_{end} \leftarrow t_{end} / \lambda_t^2$ ;
25      | Break;
26    end
27    if  $sta == 1$  then
28      | Append  $[(x_{end} - x_{start})/m, t_{end}/n]$  to result;
29    end
30    else
31      |  $t_{end} \leftarrow t_{end} \times \lambda_t^1$ ;
32      |  $counter \leftarrow counter + 1$ ;
33    end
34     $x_{end} \leftarrow x_{end} \times \lambda_x$ ;
35  end

```

Table 7. Estimated values of the parameters p_1 and p_2 of the function $p_1 \Delta x^{p_2}$

n	m	$\alpha = 1$			$\alpha = 0.75$			$\alpha = 0.5$		
		p_1	p_2	R^2	p_1	p_2	R^2	p_1	p_2	R^2
10	10	0.787	1.913	1	0.457	2.518	1	0.172	3.736	1
20	20	0.624	1.954	1	0.347	2.588	1	0.127	3.873	1
40	40	0.551	1.973	1	0.307	2.631	1	0.102	3.926	1

5. Conclusions

In this paper, two numerical methods for solving the one-dimensional fractional reaction-diffusion equation were proposed. The explicit method in testing proved to be conditionally stable. The stability condition was determined by the algorithm proposed in the paper, its form $\Delta t \leq \delta_\alpha \Delta x^{2/\alpha}$ made the numerical scheme very time-consuming for small values of α . The order of convergence of the implicit method was also estimated, which was one.

References

1. BŁASIK M., 2021, The implicit numerical method for the one-dimensional anomalous subdiffusion equation with a nonlinear source term, *Bulletin of the Polish Academy of Sciences. Technical Sciences*, **69**, e138240
2. CORONEL-ESCAMILLA A., GÓMEZ-AGUILAR J.F., TORRES L., ESCOBAR-JIMENÉZ R.F., 2018, A numerical solution for a variable-order reaction-diffusion model by using fractional derivatives with non-local and non-singular kernel, *Physica A*, **491**, 406-424
3. DIETHELM K., 2010, *The Analysis of Fractional Differential Equations*, Springer-Verlag, Berlin
4. GU X.M., SUN H.W., ZHAO Y.L., ZHENG X., 2021, An implicit difference scheme for time-fractional diffusion equations with a time-invariant type variable order, *Applied Mathematics Letters*, **120**, 107270
5. HAQ S., ALI I., SOOPPY NISAR K., 2021, A computational study of two-dimensional reaction-diffusion Brusselator system with applications in chemical processes, *Alexandria Engineering Journal*, **60**, 4381-4392
6. HUMPHRIES N.E., QUEIROZ N., DYER J.R.M., PADE N.G., MUSYL M.K., *et al.*, 2010, Environmental context explains Lévy and Brownian movement patterns of marine predators, *Nature*, **465**, 1066-1069
7. KILBAS A.A., SRIVASTAVA H.M., TRUJILLO J.J., 2006, *Theory and Applications of Fractional Differential Equations*, Elsevier, Amsterdam
8. KOSZTOŁOWICZ T., DWORECKI K., MRÓWCZYŃSKI S., 2005a, How to measure subdiffusion parameters, *Physical Review Letters*, **94**, 170602
9. KOSZTOŁOWICZ T., DWORECKI K., MRÓWCZYŃSKI S., 2005b, Measuring subdiffusion parameters, *Physical Review E*, **71**, 041105
10. LIU Y., DU Y., LI H., LI J., HE S., 2015, A two-grid mixed finite element method for a nonlinear fourth-order reaction-diffusion problem with time-fractional derivative, *Computers and Mathematics with Applications*, **70**, 2474-2492
11. METZLER R., KLAFTER J., 2000, The random walk's guide to anomalous diffusion: a fractional dynamics approach, *Physics Reports*, **339**, 1-77
12. METZLER R., KLAFTER J., 2004, The restaurant at the end of the random walk: Recent developments in the description of anomalous transport by fractional dynamics, *Journal of Physics A: Mathematical and General*, **37**, 161-208
13. OWOLABI K.M., ATANGANA A., AKGUL A., 2020, Modelling and analysis of fractal-fractional partial differential equations: Application to reaction-diffusion model, *Alexandria Engineering Journal*, **59**, 2477-2490
14. PODLUBNY I., 1999, *Fractional Differential Equations*, Academic Press, San Diego
15. PRADIP R., PRASAD GOURA V.M.K., 2023, An efficient numerical scheme and its stability analysis for a time-fractional reaction diffusion model, *Journal of Computational and Applied Mathematics*, **422**, 114918

16. SAAD K.M., GÓMEZ-AGUILAR J.F., 2018, Analysis of reaction-diffusion system via a new fractional derivative with non-singular kernel, *Physica A*, **509**, 703-716
17. SANDIP M., SRINIVASAN N., 2023, Analytical and numerical solutions of time-fractional advection-diffusion-reaction equation, *Applied Numerical Mathematics*, **185**, 549-570
18. SAXENA R.K., MATHAI A.M., HAUBOLD H.J., 2015, Computational solutions of unified fractional reaction-diffusion equations with composite fractional time derivative, *Communications in Nonlinear Science and Numerical Simulation*, **27**, 1-11
19. SOLOMON T.H., WEEKS E.R., SWINNEY H.L., 1993, Observations of anomalous diffusion and Lévy flights in a 2-dimensional rotating flow, *Physical Review Letters*, **71**, 3975-3979
20. WEEKS E.R., URBACH J.S., SWINNEY L., 1996, Anomalous diffusion in asymmetric random walks with a quasi-geostrophic flow example, *Physica D: Nonlinear Phenomena*, **97**, 291-310

Manuscript received December 27, 2023; accepted for print February 19, 2024